Article

Investigation of Foam Flooding Assisted by Non-Newtonian and Novel Newtonian Viscosifying Agents for Enhanced Oil Recovery

Seyed Mojtaba Hosseini-Nasab,* Mohammad Rezaee, Martin Taal, and Pacelli L. J. Zitha*

Read Online

ACCESS | Metrics & More | Article Recommendations

ABSTRACT: One of the main reasons for foam flooding enhanced oil recovery (EOR) is mobilizing oil left in the reservoir after primary recovery (depletion by pressure difference solely) and water flooding. However, expanding the infrastructure for certain foam EOR projects might be necessary as more wells are required, or a different well pattern is necessary. This study aims to study the effect of Newtonian and non-Newtonian viscosifying agents to assist foam flooding under the porous medium condition and to compare the results. Furthermore, this paper attempts to investigate the use of glycerol as a novel promising economic and ecological candidate instead of polymers. The shear rate inside the core was calculated based on the literature, which was combined with viscometric measurements in order to form four pairs of equal apparent viscosity. The differences and overlap within the core flooding experiments with foam generated by Newtonian and non-Newtonian fluids were observed by examining the mobility reduction factor under transient and steady-state conditions and by calculating the gas fraction present in the core. It was concluded that glycerol in core flood experiments could reach the same mobility reduction factor of about 1600 as polymer solutions with the same apparent viscosity, as long as the viscosity of the injected solution is reasonably low. Moreover, glycerol even reached the maximum mobility reduction factor faster than the foam generated by the polymer solution.
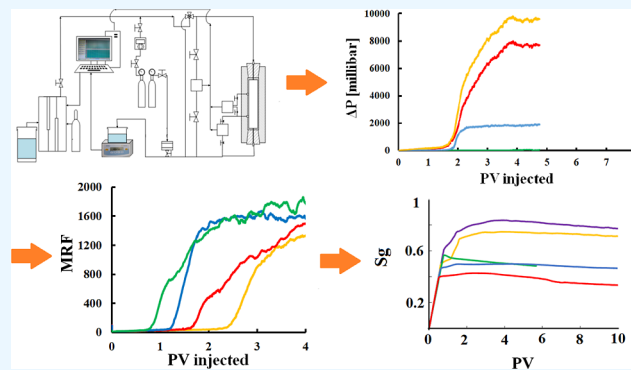
INTRODUCTION

As the reservoirs reach their final part of secondary oil recovery and also due to limited crude oil resources, companies and countries will be forced to look for other ways to preserve their market share, turnovers, or profit. Therefore, a shift toward a more efficient recovery of existing reservoirs is a logical outcome for a market that finds itself in its current state. The aim of enhanced oil recovery (EOR) is to mobilize oil left in the reservoir after primary recovery (depletion by pressure difference solely) and water flooding. Gas injection is one of the most applied techniques in EOR.[1,2] Gas injection often suffered from small volumetric (areal and vertical) sweep efficiency, resulting in the gas contacting only a small fraction of the oil present in the reservoir.[3−5] Due to its low viscosity, injected gas flows through the paths of least resistance in the reservoir, leaving low-permeable zones reservoir. On the other hand, gas and surfactant co-injection creates foam that leads to far larger mobility reduction, thus enhancing mobility control.[6,7]

During foam generation in a porous medium, gas injection into the core plug causes the process of "leave-behind", where films are formed in the pore throats as gas comes into the pore from different directions. This process only occurs when drainage is present (increasing gas fraction).[8,9] Phase separation of foam occurs as the liquid fraction of foam enters small pores in the low-permeable sections of the core as it does not require the same high-pressure gradient as the gas phase does. The gas phase invades the high-permeable regions.[10,11]

For a constant flow of a co-injected gas and liquid in a pre-flushed (with surfactant solution) homogeneous porous medium, there is a pressure gradient observed for which the generation of weak foam changes to the generation of strong foam.[12−14] The generation of strong foam drastically reduces mobility.[15,16]
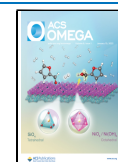
Some researchers examined the effect where the addition of a polymer to the injected surfactant solution enhances both foam viscosity and stability, and such polymer-enhanced foams (PEFs) can be used as an effective mobility control agent.[17−19]

When the bulk liquid used to generate foam contains polymers, the foam has more resistance to gas flow than foam

generated by a bulk solution without polymers.[20,21] Hanamertani and Ahmed[22] found that PEFs showed better mobility control and flow resistance, higher foam strength, and finally EOR significantly.

Gochev[23] suggested that higher foam stability could be achieved using hydrophobically modified inulin (a type of polymer) associated with the formation of larger polymer loops in the aqueous phase, leading to foam stability. Previous studies have shown that there is a correlation between bulk and core flood experiments in terms of how foam stability in the absence of oil affects this relationship.[24] Propagation of foam in porous media is affected by properties of porous media such as pore size distribution, pore shape, and pore connectivity.[25−27] When the porous medium is heterogeneous, foam behavior is further complicated due to variation in the porous structure and/or wettability.[27,28] Foam flooding has been shown to be more promising in terms of sweeping efficiency, processing time, and material consumption than other EOR processes such as water flooding, surfactant flooding, or polymer flooding.[29−31]

Although there are many benefits of using polymers for EOR purposes, some drawbacks hinder their implementation on a large scale. A polymer under harsh conditions of reservoirs like high temperature and high salinity (HTHS) degrades and loses its ability.[32,33] Furthermore, the polymer degrades and precipitates when it contacts brine ions in the reservoir, which causes clogging and reduces the permeability.[34,35] Also, the viscosity of the polymer reduces tremendously upon contacting the brine in the reservoir. Therefore, a substantially higher polymer concentration is required to achieve desirable viscosity, which increases the expenditure and financial obstacles. It should be considered that a polymer has high molecular weight and could cause formation damage. Also, polymer-assisted foam flooding is more suitable for increasing recovery of high-viscosity oil.[36−38] Hence, finding a suitable substitute instead of polymers is required tremendously.

A recent study from Hosseini-Nasab et al.[19] reports on the blend of surfactant−glycerol flooding of water-flooded sandstone cores to mobilize residual oil. The study aimed to provide an alternative approach for alkali−surfactant−polymer flooding as reservoir properties sometimes limit this method. They reported that flooding the surfactant−glycerol solution can increase oil recovery significantly. Micromodel and porous medium studies have been presented to investigate the flow properties of conventional foams and PEFs through porous media. Researchers noted that mobility control with PEF was higher than that with conventional foam due to its high viscosity and stability.[39,40]

In the previous research,[41] the performance of viscosifying agents on foam stability under bulk conditions was investigated. It was observed that both the polymer and glycerol could increase foam stability significantly. It was also concluded that the maximum liquid volume in the foam and adsorption into the foam were remarkably higher for glycerol solutions than those for a hydrolyzed polyacrylamide (HPAM) polymer.

Due to the increase in bio-based fuel usage, a substantial surplus of crude glycerol is provided in the market, which offers an interesting economic and environmental opportunity for investigating its application as a substitute for polymers for EOR.[42] On the other hand, due to the limitation of using polymers mentioned earlier such as under harsh conditions (HTHS) and low performance in the low-permeability reservoirs, glycerol can be considered a novel agent and a proper candidate which needs more studies and research to be done on it.

Therefore, this study aims to comprehend the effect of glycerol on production of strong foam in core flood tests compared to that of polymers and also gain a deeper understanding of these viscosifying agents in foam flow behavior in porous media. In order to compare, experiments are performed with Newtonian and non-Newtonian viscosifying agents with different concentrations. To this end, the rheology and shear rate are aimed to be investigated and analyzed inside the core, clarifying their impact on foam performance in the porous media and guiding them to modify and optimize the implementation of foam in EOR processes.

Rheology inside Porous Media. The rheological behavior of non-Newtonian HPAM solutions in flow through a porous medium is of significance. The rheology involves the observation of how properties vary when shear stress and time increase. For Newtonian fluids, $\sigma = \eta\gamma$ holds. In theory, foams can consist of a homogeneous structure, but in experiments, foams are usually heterogeneous, making the determination of foam rheology hard. Added to this is the compressibility that comes into play for foams at high flow rates and pressures, which makes foam rheology a difficult subject to measure.[43−45] Therefore, in this study, the rheology of the fluids which will generate the foam is examined, and pairs are made based on their apparent viscosity.

The study of the flow behavior of the injected fluids in a viscometer is linked to the core flooding, but the behavior is not the same and not completely related. The flow inside the rheometer is a simpler environment than the tortuous flow inside a core/porous medium. For non-Newtonian fluids like polymer solutions, the viscosity is a function of the shear rate. HPAM is a polyelectrolyte (polymers which have several charges at the length of the chain), so the salt concentration has a large effect on the viscosity, as the ions in the solutions interact with the charges in the chain.[46] The charged body forms an electrical double layer with its oppositely charged ions, called a cloud.[47,48] These clouds can overlap when multiple charged bodies come into each other's vicinity, leading to a high concentration of the specific ion locally, increasing the osmotic pressure locally, which draws the solvent to that specific area causing increased disjoining pressure.[48,49] The size of the double layer is related to the ionic strength; a high salt concentration leads to lower disjoining pressure. This means that the flexible coils are compressed at high salt concentrations, and the resulting smaller molecule decreases the viscosity.[50]

In bulk experiments, the polymer concentration is thought to be constant throughout the solution. However, flow in porous media is different; a lower concentration of the polymer is present in the near-wall area inside narrow channels.[51,52] The molecules in the middle can move and rotate more freely than the molecules which are restricted by the nearby wall, leading to a larger concentration in the middle of the channel where the velocity is higher. Hence, the viscosity of the bulk solution increases further away from the wall.[53,54]

There have been several slightly varying expressions established in the literature in order to relate experimental conditions to the shear rate in the porous medium. Most findings have been done in experiments regarding the flow of xanthan in porous media, based on a capillary bundle model which overestimates the viscosity and underestimates the shear

rate. The effective shear rate in the porous medium is defined as follows.[55,56]

$$\dot{y}_{pm} = \alpha' \times \frac{4u}{\sqrt{8 \times k \times \phi}}$$

where α' is defined as the shape parameter that characterizes the pore structure compared to the situation where all capillaries have the same diameter (where $\alpha' = 1$), u is the Darcy velocity, k is the permeability, and ϕ is the porosity.

The situation becomes more complex when a polymer such as HPAM is used instead of xanthan, which exhibits viscoelastic properties. While xanthan shows a Newtonian behavior for low shear rates and shear thinning for higher shear rates, the behavior for HPAM goes from Newtonian to shear thinning to eventually shear thickening for high shear rates.[52] Therefore, the effective shear rate definition established for xanthan-like polymers cannot be substituted into an HPAM formulation that easily. Another aspect is the event of degradation of HPAM at high shear rates. However, Sorbie[57] concludes that for low flow rates, these additional factors do not play an important role, and therefore, the same formulation as that described above for xanthan can be applied to the HPAM polymer. A combination of HPAM polymers and a biopolymer was also investigated.[58] They observed that the viscosity of HPAM tended to increase at a specific apparent shear rate, which was not observed for biopolymers. These results indicate the thickening of the flow in the porous medium. Figure 1 represents the apparent viscosity of the HPAM polymer at different shear rates.
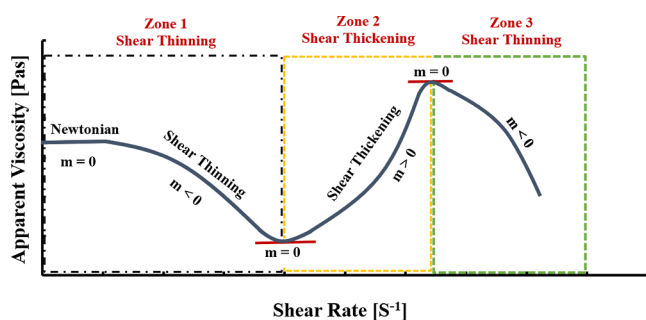

Figure 1. HPAM apparent viscosity behavior vs shear rate. Shear thickening response of HPAM at a high shear rate.

Therefore, this study aimed to relate the viscometry measurements to the rheology by establishing an expression of the shear rate inside the core. In order to compare core flood experiments performed with Newtonian and non-Newtonian viscosifying agents, the aim is to compare fluids with different rheological properties but at equal viscosities. It is therefore necessary to establish the apparent viscosity of the solutions for the shear rate present in the core.

■ EXPERIMENTAL DESCRIPTION

Experimental Setup. The determination of foamability and foam stability in porous media is done by using a core flooding setup. Bentheimer cores are used with dimensions of 17 cm length and 3.9 cm diameter. The porosity of cores was measured using porosity meters which worked with helium gas. To measure the permeability of cores, brine with different rates was injected in the cores, and pressure drops were recorded,

and with the Darcy law, the permeability was calculated. Specification of the core properties is given in Table 1.

Table 1. Physical Properties of Core Samples Used for Flooding Experiments

core sample	Bentheimer sandstone
length [cm]	17.0 ± 0.1
diameter [cm]	3.9 ± 0.1
porosity [%]	23
pore volume [cm^3]	46.7
absolute permeability to brine [Darcy]	3.1 ± 0.12 (core 1) and 2.8 ± 0.12 (core 2)

The Bentheimer cores are often used for oilfield research due to their homogeneity in both grain size and pore size distribution.[59] After the cores are drilled from a larger cubical block, they are sawn into the dimensions described above. Preparation of the cores consists of drying to evaporate any liquid present inside the cores. To ensure that the flow during the experiments is purely in the vertical orientation of the core, flow from the side of the core must be prevented. This is done by applying a thin layer of glue to the core, which prevents penetration. Two holes were drilled into the core which will be used for pressure measurements during the experiments. The core is then placed inside the core holder. The core holder is made of an organic polymer, polyether ether ketone. Two pressure transducers are connected to the holes drilled in the core to measure the pressure difference between two sections of the core. A third pressure transducer measures the overall pressure drop of the whole core length. For all experiments, a back pressure of 30 bar is applied.

Foam is generated inside the core by co-injection of gas and surfactant solution at the top of the core. The gas flow rate is set by applying a fixed gas flow rate with a mass flow controller. The gas used in the experiments is nitrogen with a purity of 99.98%. A Quizix pump is used to implement a fixed liquid flow rate. All experiments contain 1.0 wt % sodium chloride (NaCl, purchased from J.T.Baker), dissolved in demineralized water. The surfactant used to stabilize the foam was α-olefin sulfonate C_{14-16} (AOS C_{14-16}, Stepan, active content 39%). The polymer which was used for all experiments was partially HPAM (FLOPAAM 3530s from SNF Floerger), and the glycerol Anhydrous Biochemica was purchased from Applichem Panreac. All experiments were conducted at room temperature.

The mass of the effluent is measured by placing a balance (Sartorius) at the outlet. The balance is connected to a computer to obtain the mass produced in real time. Pressure data was recorded and displayed in real time on the monitor connected to the computer.

In order to study the properties of foams in porous media, a core flooding setup is constructed, which is shown in Figure 2.

Experimental Procedure. The first step in the preparation of the core for the experiments was flushing the core with CO_2 at a back pressure of 5 bar. This was done to remove any air inside the core. The back pressure was then increased to 35 bar, and brine was injected for 5 pore volumes (PVs) at 1 mL/min. The high pressure is needed to dissolve CO_2 present in the core in the injected brine. After this injection phase, the core was fully saturated with brine. The permeability was determined at 25 bar back pressure by injection of brine at different flow rates while measuring the pressure drop.
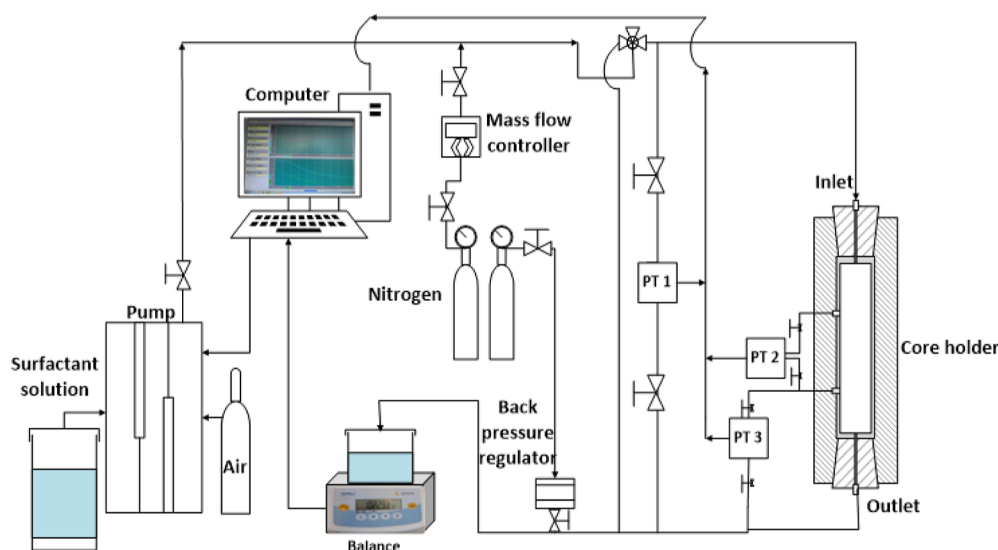
Figure 2. Setup used in the core flooding experiments.

For each experiment, the core was pre-flushed with 5 PV of the solution that would be used in the specific experiment. The pre-flush volume ensures that adsorption of the specific substances in each solution is met and the shortening of the time of foam generation in the co-injection phase. The foam quality is fixed at 82%, and the total flow rate is 0.55 mL/min. Table 2 gives an overview of the steps taken during core flood experiments.

Table 2. Sequence of Steps Taken during Core Flood Experiments

step	description	back pressure [bar]	surfactant concentration [wt %]	total flow rate [mL/min]	foam quality [%]
1	CO_2 flushing	5			
2	core saturation	35		1	
3	pre-flush	30	0.5	2	
4	co-injection	30	0.5	0.5	82

The first core was used to examine the foam floods with glycerol in increasing concentrations. The second core was subjected to polymer-assisted foam floods in increasing concentrations. After cleaning and repeating the first polymer experiment to confirm that the same pressure drop was achieved, polymer—glycerol solutions were injected at increasing concentrations. An overview of the experiments which were performed is shown in Table 3.

◼ MATERIALS AND METHODS

All experiments in the liquid phase contain 1.0 wt % sodium chloride (NaCl, purchased from J.T.Baker, The Netherlands), dissolved in demineralized water. The gas source used for foam generation was nitrogen, and the gas flow rate was measured with a built-in mass flow meter during the experiment. The surfactant used to stabilize foam was AOS C_{14-16} (Stepan, Belgium, active content: 39%). In this work, 0.5 wt % AOS C_{14-16} is used in all experiments since the study from Vikingstad[60] showed that for AOS C_{14-16}, no increase in foam height was noticed when the surfactant concentration

Table 3. Overview and Sequence of Core Flooding Conducted Experiments

	core plug 1		core plug 2	
experiment	glycerol [wt %]	polymer [ppm]	glycerol [wt %]	polymer [ppm]
1	0	150	0	150
2	20	250	0	250
3	30	450	0	450
4	40	750	0	750
5	50	150	0	150
6	60	250	40	250
7			50	250
8			60	450

was increased from 0.5 to 1.0 wt %. The polymer which was used in the experiments was a partially HPAM (FLOPAAM 3530s from SNF Floerger, France). The degree of hydrolysis of this specific HPAM was between 25 and 30%. The glycerol anhydrous BioChemica was provided by AppliChem PanReac, The Netherlands.

Foam Core Flood Test. In core flooding experiments, the porous medium is first saturated with a surfactant solution after which co-injection of the surfactant solution and nitrogen takes place to create in situ foam. The reason for pre-flushing the core with surfactant solution is to compensate for rock surface adsorption, while it also speeds up the foam generation since the surfactant is already in the system when gas is injected. As the core is saturated with the surfactant solution, gas injection into the core causes the process of "leave-behind", where films are formed in the pore throats as gas comes into the pore from different directions.[9] This process only occurs when drainage is present (increasing gas fraction).

In the core flood experiments, a total flow rate of 0.55 mL/min is measured when co-injection of gas at a flow rate of 0.45 mL/min and liquid at a flow rate of 0.1 mL/min is applied. The following parameters are calculated in order to determine the range of possible shear rates in the core flood experiments. With $\alpha'\varepsilon$ (3.0,5.0), the shear rate is calculated to be in the range of (38/s, 63/s).
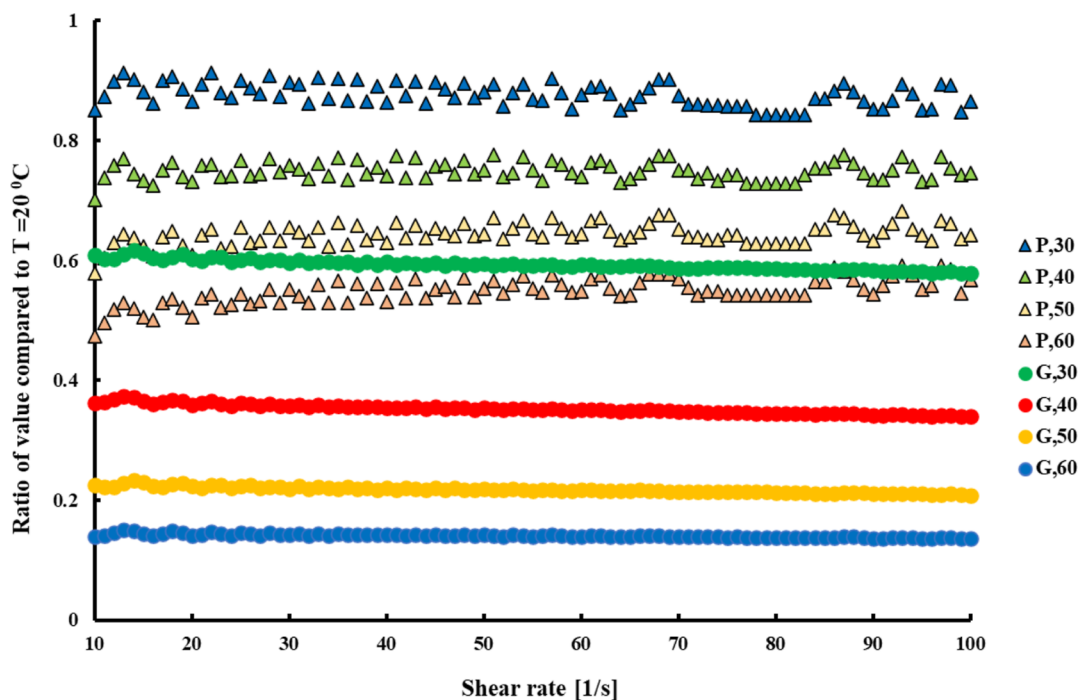
Figure 3. Normalized apparent viscosities for 85% glycerol and 1000 ppm HPAM solutions. With increasing the temperature, the normalized viscosity of both the glycerol and polymer decreases.
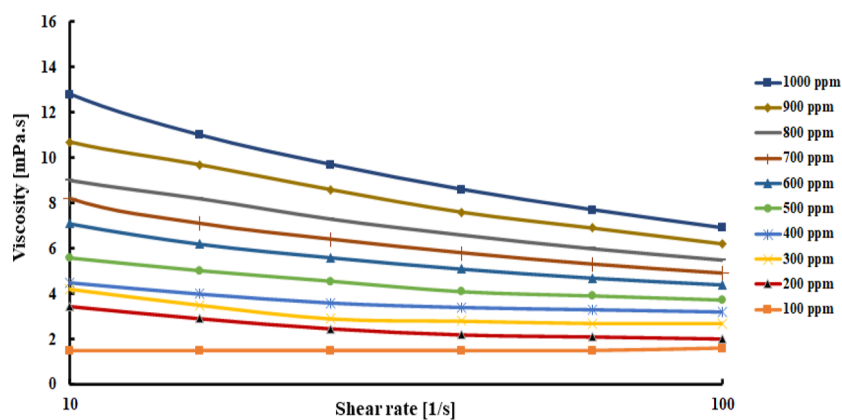

Figure 4. Measured apparent viscosity for a range of HPAM concentrations in the shear rate domain of [10/s to 100/s]. By increasing the shear rate, viscosity decreases. For higher concentrations, the decrease is higher compared to that at lower concentrations.
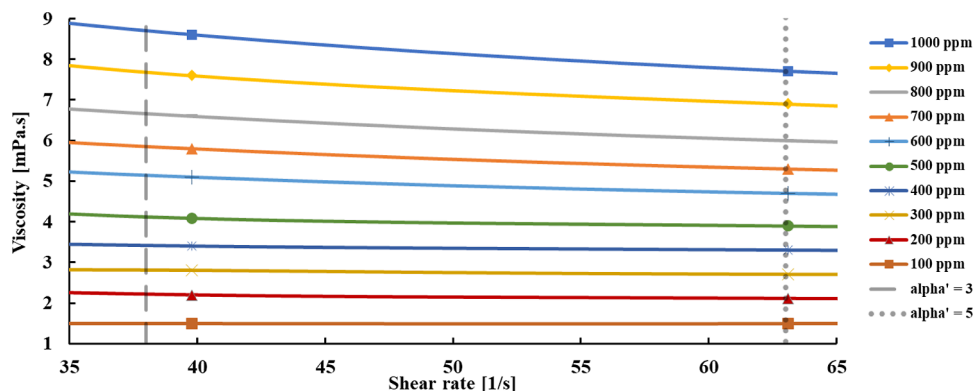

Figure 5. Measured apparent viscosity for a range of HPAM concentrations in the shear rate domain estimated to have occurred in the core flooding experiments.
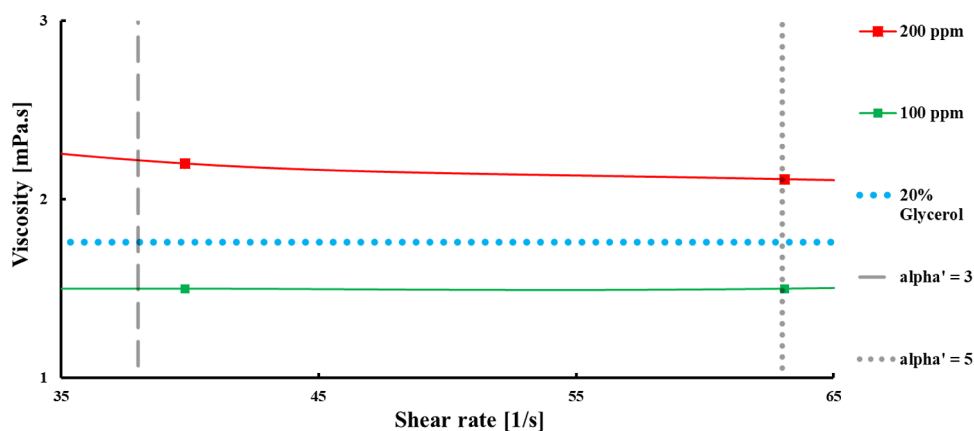
Figure 6. Matching of the apparent viscosity of the 20% glycerol solution with that of HPAM solutions. As it suggests, parameter α' has no effect on the apparent viscosity in this domain, and no shear thinning can be observed.
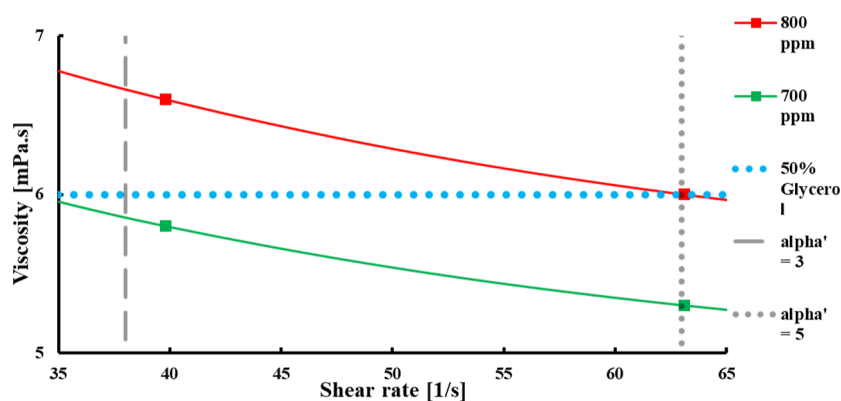

Figure 7. Matching of the apparent viscosity of the 50% glycerol solution with that of HPAM solutions. As the figure indicates, at 50% glycerol, parameter α' has a significant effect on apparent viscosity, and more shear thinning can be observed.

■ RESULTS AND DISCUSSION

First, the temperature sensitivity was measured for an 85% glycerol sample and a 1000 ppm HPAM sample. Both experiments are performed with 1.0 wt % NaCl and the 0.5 wt % surfactant. The effect of the increase in temperature on the viscosity of glycerol and polymer solutions is shown by normalizing the initial value so that purely the effect of temperature becomes visible. This is done by displaying the apparent viscosities at a higher temperature as the fraction of the apparent viscosity at $T = 20$ °C which is shown in Figure 3.

When the liquid is in a high-temperature environment, the molecules of the liquid have more energy and spread further apart. This enables the molecules to move around much more in the liquid, making it less viscous. It is quickly observed that a temperature increase affects the viscosity of the 1000 ppm polymer solution much less than that of the 85% glycerol solution, for which the rise of the temperature from 20 to 60 °C makes the viscosity drop by 85%. For the polymer solution, this is only 45%. This is an aspect that is important to consider for application in the field where reservoir conditions (with a temperature range of 80 to 130 °C) will often be in the higher range of the temperatures that were tested here.

Ten samples ranging from 100 ppm HPAM to 1000 ppm HPAM were prepared in a 1.0 wt % NaCl solution to determine the apparent viscosity for the shear rate. The device used is the Anton Paar MCR rheometer, and all measurements are performed at $T = 20$ °C. The viscosity measurements are shown in Figure 4, where the shear thinning can be clearly

observed. This means that the assumption that the formulation for the xanthan polymer can be applied here for the HPAM polymer under these conditions is correct since no shear thickening occurs at these shear rates.

A closer look at the shear rate domain of 38/s to 63/s shown in Figure 5 shows the almost Newtonian behavior for the lower concentrations of HPAM, while the higher concentrations of HPAM still show quite some shear thinning. The lack of rigidity of the molecule causes the molecule to be pulled apart when high elongational stresses are present.[57] This means that the choice of the value for α' is more important for the higher-viscous solutions, while the viscosity of less-viscous solutions is more indifferent to α'.

In order to compare Newtonian fluids with non-Newtonian fluids according to their apparent viscosity at the shear rate of the porous medium during the core flood experiments, the viscosity of glycerol solutions is added to the figure. To avoid having one figure with too much data, the choice is made to present one figure per glycerol solution with the HPAM solutions added. These figures form the basis of the decision of which glycerol concentration should be compared with which HPAM concentration in the core flood experiments. Figures 6 and 7 show the results of the measurements for glycerol concentrations of 20 and 50%, respectively. For the 20% glycerol solution, the HPAM solutions, which exhibit similar apparent viscosities, show almost no shear thinning in this shear rate domain. Therefore, the empirical parameter α' is not of great importance here, and the approximation of the match

is accurate. An HPAM concentration of 150 ppm corresponds well with the 20% glycerol solution.

As it can be observed in Figure 7, for the more viscous 50% glycerol solution, the HPAM solutions which exhibit similar apparent viscosities show far more shear thinning in the shear rate domain. Here, the value of the empirical parameter α' has a far greater influence on the expected apparent viscosity of the solutions in the core flooding experiments. Therefore, the accuracy of the expected apparent viscosity of the HPAM solution is lower. An HPAM concentration of 750 ppm corresponds on average with the 20% glycerol solution.

Table 4 shows the concentrations of HPAM and glycerol which are matched based on their apparent viscosity for the expected shear rate inside the core.

Table 4. Glycerol−HPAM Pairs Based on the Apparent Viscosity Expected during the Core Flood Experiments

pair	surfactant concentration [wt %]	glycerol concentration [wt %]	polymer concentration [wt %]
1	0.5	20	150
2	0.5	30	250
3	0.5	40	450
4	0.5	50	750

The control experiment is experiment 1 of core 1 which is presented in Table 3. The results of this core flood are summarized in Figures 8 and 9. The pressure difference over the core's middle section, over the core's outlet section, and over the whole core length is measured using the pressure transducers, as shown in Figure 2. The pressure of the entry section is calculated by subtracting the pressure difference over the middle and outlet sections from the pressure difference over the core. A very small pressure difference is found to exist in the entry section of the core, which shows no significant change with time. The pressure difference over the outlet section develops the latest as the foam propagates initially from the inlet toward the outlet of the core. However, after ±1.7 PV, the pressure difference over this section increases and reaches a steady state shortly after 2 PV is injected. At this time in the experiment, the steady state is not yet reached in the other sections of the core.

As the foam propagates from the inlet toward the outlet of the core, a pressure buildup occurs throughout the core. This is depicted in the onset of Figure 9 for the early stage of the co-injection, up to 1.5 PV. For 2 PV injected, the increase over the outlet section shows a sharper increase in pressure drop than that over the middle section of the core. In the time between 1.5 PV and 2 PV injection, foam propagation reaches the end of the core, after which a significantly larger pressure drop occurs. This matches the data plotted in Figure 8.

Glycerol Core Floods. The results of the core floods with solutions containing glycerol show two distinct regimes regarding the maximum pressure difference over the core. For the control experiment and for the experiments containing 20 and 30% glycerol, a high-pressure drop was observed after several hours of co-injection. However, for higher glycerol concentrations of 40, 50, and 60%, the occurrence of a high-pressure drop was absent. This result is shown in Figure 10. For the core floods where the high-pressure drop did occur, the addition of glycerol showed an increase in the maximum pressure drop. A strong foam could not be developed with the solutions of 40% glycerol or higher.

Polymer Core Floods. The results of the polymer core floods show that for all concentrations of HPAM, a high-pressure drop was observed and that strong foam had developed, see Figure 11. No limitation of the HPAM concentration was found in this range of 150−750 ppm for the experimental conditions previously described.

As the aim of these experiments was to compare the glycerol and HPAM core floods based on an equal apparent viscosity, the results leave only two series of experiments for complete analysis as the higher concentrations of glycerol did not create strong foam. It can be seen in Figure 12 that the comparison based on apparent viscosity seemed to be accurate. Both pairs are close to identical in the maximum pressure drop observed. This outcome leads to the conclusion that when the maximum pressure drop is considered for relatively low apparent viscosities, there is a little difference between foams generated by Newtonian and non-Newtonian viscosifying agents.

Glycerol−Polymer Core Floods. In addition to the core floods containing only the glycerol or polymer, experiments were conducted where glycerol was added to a 250 ppm
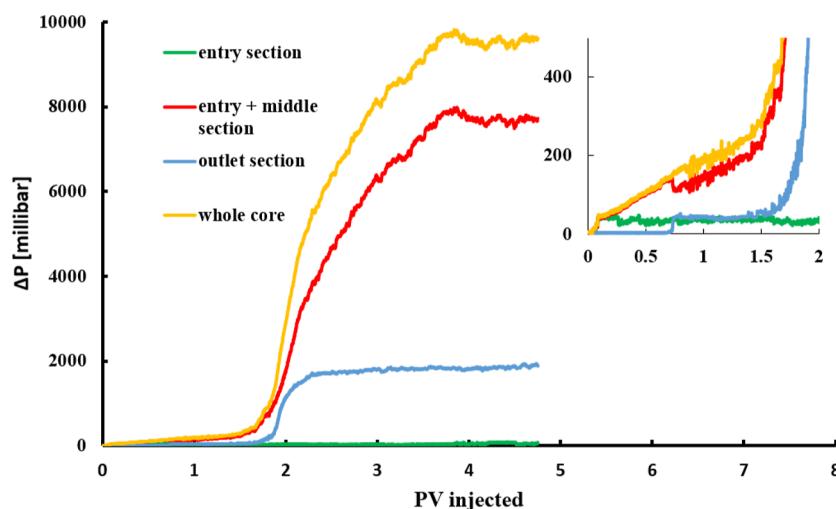

Figure 8. Sectional pressure drops for the control experiment vs the PV injected. The figure suggests that in the entry section, no significant pressure drop is observed. However, in the other section till 2 PV injection, a notable pressure drop is observed.
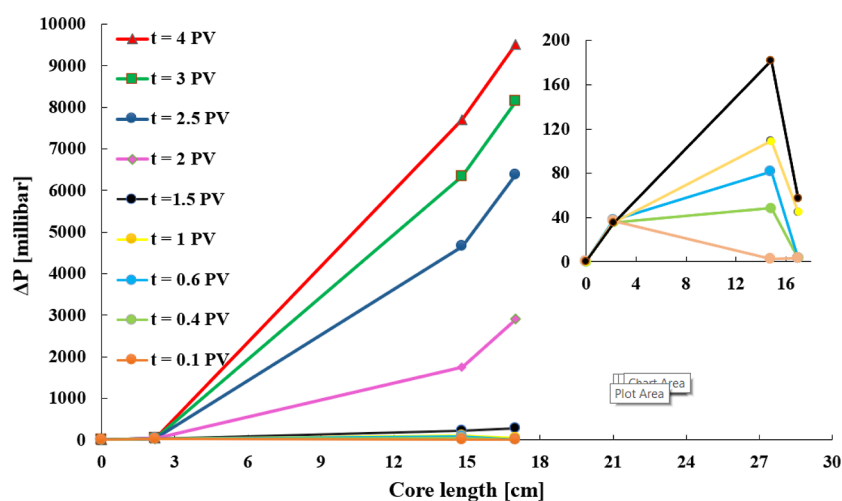
Figure 9. Sectional pressure drop vs the core length, for two different foam regimes. First, the foam propagates from the inlet toward the outlet (onset), after which the pressure drop increases drastically starting at the outlet (inset).
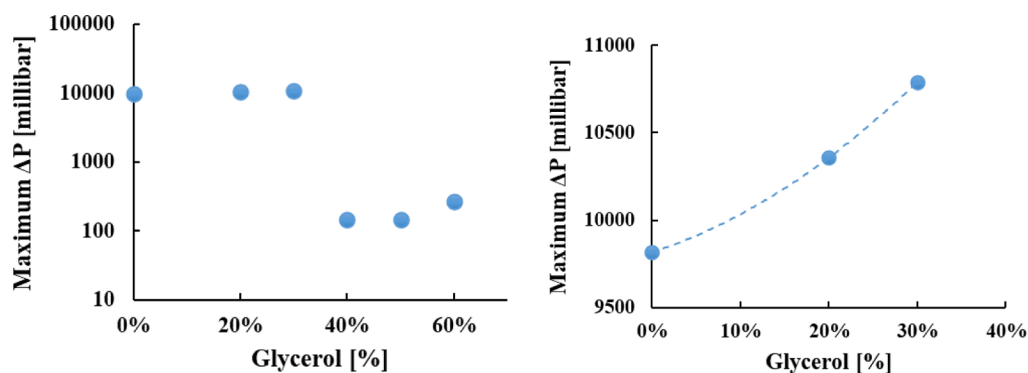

Figure 10. Maximum pressure drop over the whole core length was obtained for all glycerol experiments (left) and for the experiments containing up to 30% glycerol (right). For concentrations above 40% of glycerol, pressure drop decreases significantly compared to that for lower concentrations. However, for concentrations lower than 30%, by increasing the glycerol concentration, the pressure drop increases.
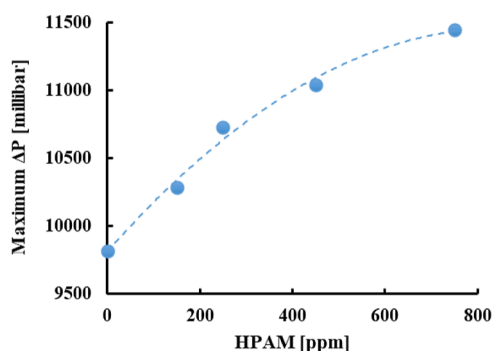

Figure 11. Maximum pressure drop over the whole core length obtained for all HPAM experiments. It indicates that by increasing the HPAM concentration, its pressure drop also increases, which is not similar to the glycerol trend.

Figure 12. Comparison of the maximum pressure drop over the whole core length for the pairs of glycerol−HPAM. According to the figure, both Newtonian and non-Newtonian agents show similar pressure drop.

HPAM solution. More precisely, the glycerol concentrations which were added were 40 and 50%. These concentrations were chosen based on the failure to generate strong foam in the previous experiments. Therefore, these experiments can help us understand why the previous experiments did not generate strong foam for glycerol concentrations of 40% or higher. In Figure 13, it is shown that the addition of 40 and 50% glycerol to a solution of 250 ppm HPAM, in fact, does generate strong foam. The maximum pressure drop is much
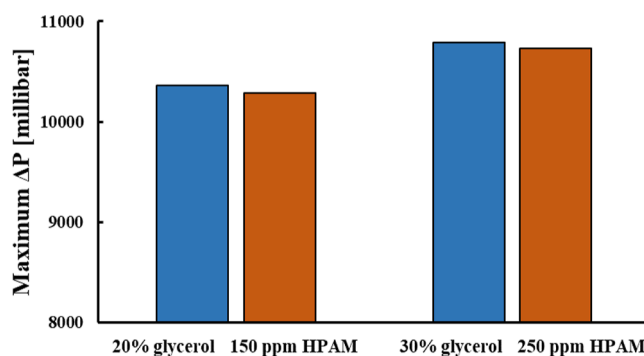
higher than that for a solution with only 250 ppm HPAM and is also much higher than that for the experiment with 30% glycerol. These results point toward a type of mechanism on a microscale which shows that the presence of HPAM increased the foamability of the solution. It could be related to the blockage of gas flow paths at the pore throats by the large HPAM molecules. If a specific concentration of glycerol would block the surfactant molecules from stabilizing the film, it could be the reason why strong foam is not generated.
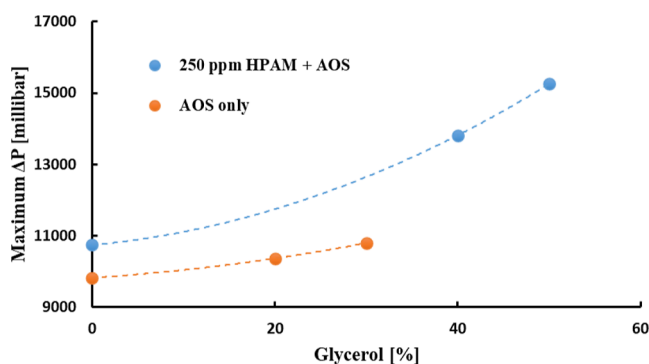
Figure 13. Comparison of the maximum pressure drop over the whole core length obtained for foam generated by solutions with and without the addition of 250 ppm HPAM. As it suggests, the AOS surfactant with 250 ppm HPAM significantly increases the pressure drop compared to the AOS surfactant solely, which leads to more stable foam in porous media.

However, then no strong foam should be able to be generated for the experiments with both the polymer and glycerol. Thus, the generation of strong foam is aided by the presence of the polymer. It could be that the drainage rate of the liquid out of the foam is essential here, as the bulk experiments showed that the liquid drains out of foam generated by a glycerol solution much faster than out of an HPAM solution.[41] Therefore, it could be that there is a lower limit of the liquid content in the foam for which strong foam can be generated and that this lower limit is not reached in the glycerol experiments with 40% and higher.

Pressure Resistance across the Core Plug. The propagation of the strong foam through the core is observed by analyzing the pressure data for the different core sections. First, the entry section is observed. For all glycerol experiments, including the 20 and 30% glycerol experiments where strong foam was generated, no significant pressure buildup was present in the time span of these experiments. As can be observed in Figure 14, for the polymer solutions, a pressure
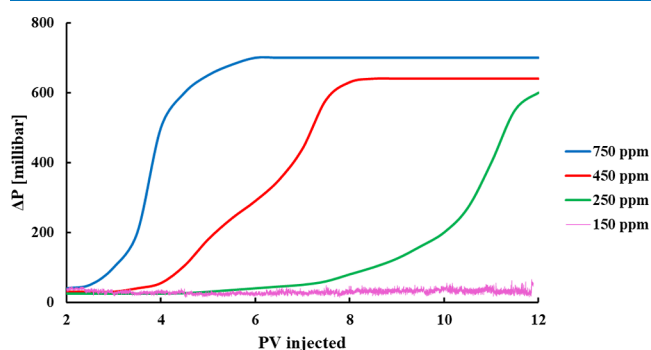

Figure 14. Pressure drop over the entry section of the core vs the PV injected for a foam generated by a range of HPAM concentrations.

buildup over the entry section was observed for 250, 450, and 750 ppm HPAM. The higher the concentration, the less the PV needed to be injected before a steady state was reached.

The experiments where glycerol is added to the 250 ppm HPAM solution show the same trend as the polymer experiments, as shown in Figure 15, the more viscous the solution is, the higher the pressure drop over the entry section. By increasing viscosity, the viscous forces between foam and
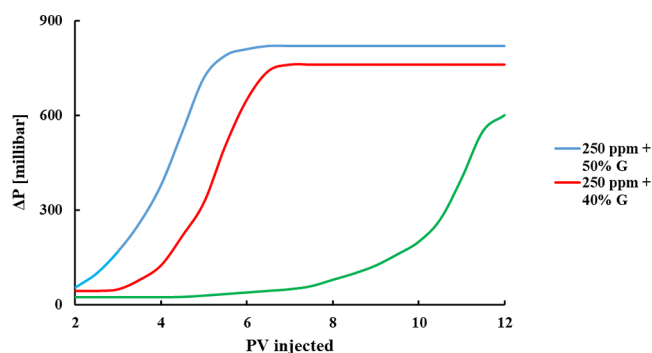

Figure 15. Pressure drop over the entry section of the core vs the PV injected for foam was generated by a 250 ppm HPAM solution with and without glycerol. As the result indicates, pressure drop over the entry section by adding glycerol increases tremendously compared to that caused by 250 ppm HPAM alone.

the porous medium increase, which results in the holding up of foam bubbles and a higher pressure drop.[62] The amount of PV injected until the new steady state is reached also decreases rapidly as the viscosity of the injectant increases.

Next, the results regarding the outlet section are examined. An interesting observation is the fact that the increase in the pressure drop does occur for the glycerol experiments here, in opposition to the lack of strong foam generation in the entry section. For increasing viscosity, the pressure drop in the steady state is higher, as expected. Another important observation which is observed in Figure 16 is that the increase
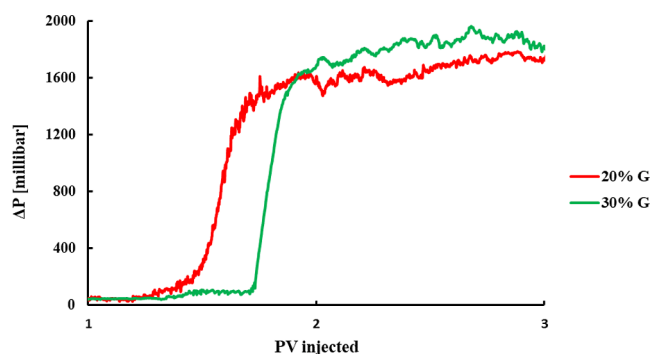

Figure 16. Pressure drop over the outlet section of the core vs the PV injected for a foam generated by 20 and 30% glycerol solutions. It indicates a trend that an increase in the glycerol concentration leads to a delay in the generation of a strong foam at the outlet section.

in the pressure drop occurs later for the more viscous solution of 30% glycerol compared to that for the 20% glycerol. For the experiments with 40, 50, and 60% glycerol, no increase in pressure drop was observed at all, which points to the fact that no generation occurs for a certain glycerol concentration.

In Figure 17, the pressure drop at the outlet section is shown for the polymer experiments, where the trend is the opposite of the glycerol trend, and an increase in the polymer concentration leads to a faster-occurring pressure drop and generation of strong foam. This supports the assumption that the presence of the polymer increases the foamability of the solution. This occurrence can be a result of slower gas diffusion and liquid drainage from foam bubbles because of higher viscosity.[61] In Figure 17, only the pressure drop development is shown until it reaches its steady state to avoid various curves crossing each other and making the figure harder to read. The
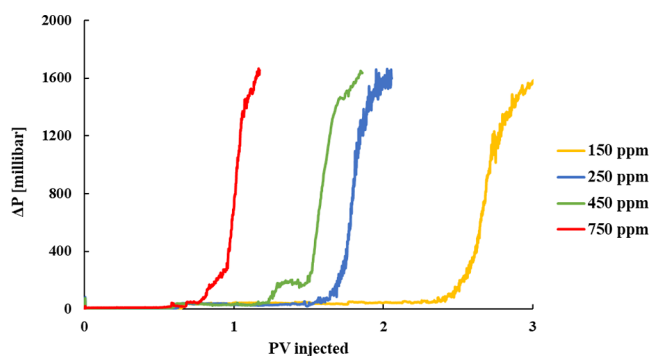
Figure 17. Pressure drop over the outlet section of the core vs the PV injected for foam is generated by a range of HPAM concentrations. The figure demonstrates that higher concentrations of HPAM reach higher pressure drop with fewer PV injected compared to lower concentrations.

final equilibrium pressure drop for the outlet section increases slightly as the HPAM concentration increases.

For the whole core length, the mobility reduction factor (MRF) against the PV injected is depicted in Figure 18. The
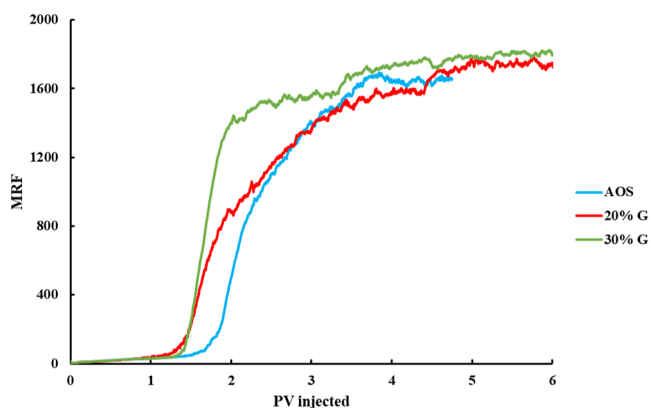

Figure 18. MRF over the whole core vs the PV injected for foam generated by solutions containing 0, 20, and 30% glycerol. According to the figure, the pressure development starts after injection of 1.4 PV, while for the outlet section, the pressure drop starts to increase for 1.5 PV and 1.8 PV. This points to the start of the generation of strong foam occurring in the section before the outlet section and propagating toward the outlet section.

MRF presents the ratio of the maximum pressure drop achieved by foam injection to the maximum pressure drop achieved by brine injection at the same total flow rate. For the glycerol experiments, the increase in the glycerol concentration led to a faster state of equilibrium and a higher MRF, but it was limited to a maximum of 30% glycerol as the higher concentrations did not generate strong foam. It is interesting to compare the time where the increase in the pressure drop starts to develop for the whole core length to the starting time of development at the outlet section.

The polymer experiments show the same behavior here as the glycerol experiments, where an increasing concentration of the polymer leads to faster development of the pressure drop over the whole core length. As can be seen in Figure 19, the MRF is higher for the more viscous solution in a steady state after the strong foam is generated. When the times where the increase in the pressure drop starts to develop for the whole core length and the outlet section are compared, it confirms
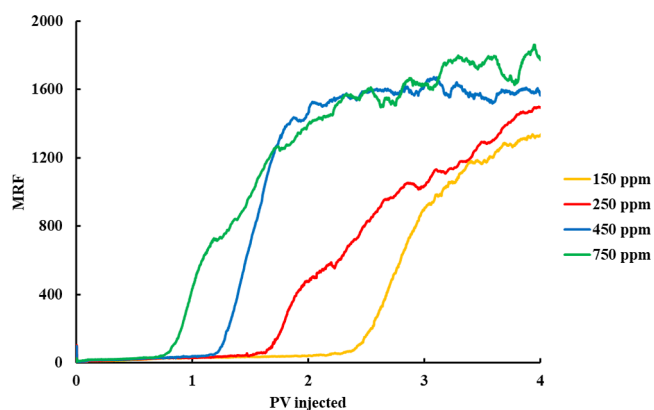

Figure 19. MRF over the whole core vs the PV injected for foam generated by a range of HPAM concentrations. As the figure indicates, since the equilibrium is reached much later in the inlet section and a bit later in the outlet section, the assumption is made that the strong foam starts to develop in the midsection, propagates toward the outlet section, and then propagates back toward the inlet section.

the idea postulated previously that the generation of strong foam occurs before it does in the outlet section and propagates to the outlet section. Since the polymer core floods also showed an increase in the pressure drop for the inlet section, a comparison can be made between the three sections.

Finally, the comparison of the previously determined couples of glycerol and HPAM solutions is shown in Figure 20. It seems that the decision to compare foams generated by solutions with an equal apparent viscosity is justified. For both comparisons, the same maximum MRF is reached, but in both cases, the glycerol solution develops the strong foam earlier than the HPAM solution does. This means that a smaller volume of solution and gas has to be injected in order for the same MRF over the whole core to be reached. This could have economic advantages when applied to a real production field.

Gas Fraction Development in Time. In order to investigate the results further, an analysis is made of the gas fraction in the core during the experiment. This is done by applying the concept of conservation of mass. At the time t_0, taken as the moment the co-injection of gas and solution reaches the entry of the core, there is a certain amount of mass present in the core. Since the core is fully saturated by the pre-flush solution, this mass is given by the density of the solution times and the PV. To complete the mass balance equation, the input must be known, which is the product of the fluid's density, the fluid's flow rate, and the injection time. The output is measured using a scale at the outlet. This mass balance equation presents the liquid saturation S_l in the core, which gives the gas saturation S_g ($S_g = 1 - S_l$).

The glycerol experiments in Figure 21 all show a sharp increase for S_g at the beginning of each experiment, after which the gas saturation becomes more or less steady or slowly decreases. In the experiments where the strong foam is developed, the 20 and 30% glycerol solutions show a maximum gas saturation of 0.82 and 0.73, respectively. On the other hand, the solutions that were not capable of generating strong foam reach far less maximum gas saturation. This implies that rather than the gas displacing a great amount of the fluid present and creating foam, it only displaces a bit of fluid. This could be explained by the concept earlier described where the weak foam is present but does not block all flow paths of the gas. It also explains why the solution of 20% glycerol develops
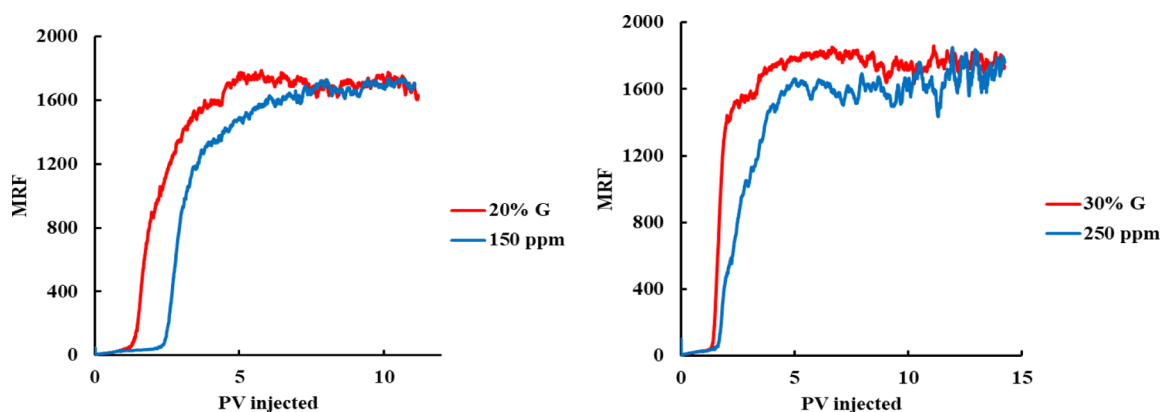
Figure 20. Comparison of the MRF vs PV injected of pair 1 (left) and pair 2 (right). As the figure suggests, both the pairs reached the similar MRF after several injections. However, in both cases, glycerol reached stronger foam faster than HPAM.
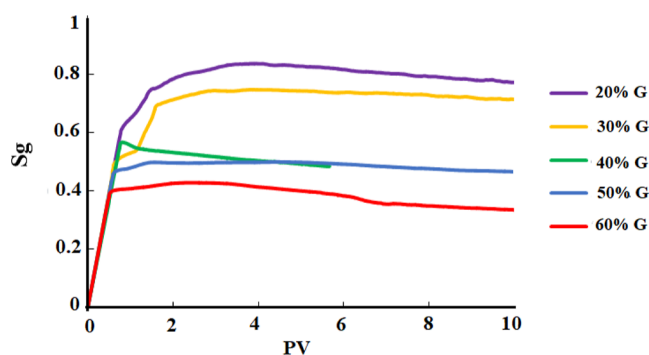

Figure 21. Gas fraction inside the core vs the PV injected for foam generated by a range of glycerol concentrations. According to the result, solutions with higher glycerol concentrations have less S_g compared to those with lower concentrations of glycerol. It indicates that lower concentrations of glycerol are able to displace liquids in the core.

Figure 22. Pressure drop over the whole core vs the gas fraction inside the core for foam generated by 250, 450, and 750 ppm HPAM. As the figure suggests, higher concentrations of HPAM could generate strong foam at lower S_g compared to lower concentrations.

Figure 23. Pressure drop over the whole core vs the gas fraction inside the core for foam generated by 20 and 30% glycerol. It indicates a trend that an increase in the glycerol concentration leads to generation of a strong foam at lower S_g.

the strong foam earlier than the 30% glycerol solution does; namely, more gas is inside the system, and therefore, it creates more strong foam sooner, while the more viscous solution of 30% glycerol is more resistant to drainage and contains more liquid throughout. This is also in accordance with the results of the bulk foam experiments, where a higher glycerol concentration led to an increase in the liquid uptake in the foam.

The comparison of the gas saturation at which the steep increase in the pressure drop over the core begins (which states the generation of the strong foam) shows that more viscous solutions can generate strong foam at a much lower gas saturation. This is the case for both the polymer and glycerol experiments as seen in Figures 22 and 23, respectively.

■ CONCLUSIONS

In this research, a polymer and glycerol (as a novel foam assisting agent) were investigated and compared. The rheology of foam flow in porous medium was examined in order to understand the mechanisms that play a role in the different behavior of Newtonian and non-Newtonian fluids under shear stress. Based on previous research described in the literature, the shear rate inside the core was calculated. Since the literature described a range for one fitting parameter, the outcome of the calculation was a range of shear rates. The apparent viscosity of the non-Newtonian solution was matched
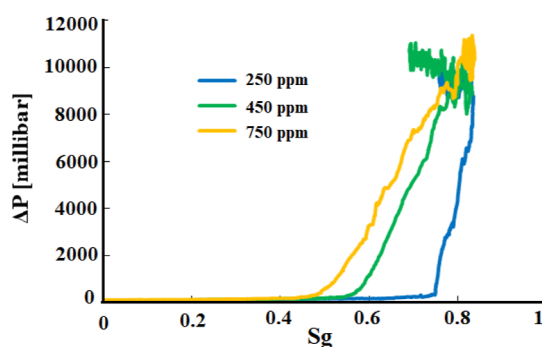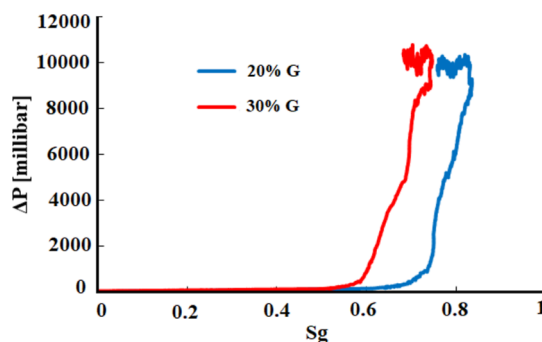
with the viscosity of the Newtonian solutions within this range of possible shear rates. This led to the formation of four pairs which were to be examined in core flood experiments.

- The experiments with glycerol showed two distinct regimes regarding the maximum pressure difference over the core. For the experiments containing 20 and 30% glycerol, strong foam was generated. However, for higher glycerol concentrations of 40, 50, and 60%, the occurrence of a high-pressure drop was absent, and a strong foam did not develop.

- For all the polymer experiments, strong foam was generated. Therefore, for the higher-apparent viscosity pairs, only the polymer led to the generation of strong foam.

- For the lower-viscous pairs, the MRF was found to be nearly identical for the foam generated by a Newtonian fluid and a non-Newtonian fluid. The Newtonian fluid generated the strong foam faster than its equally viscous non-Newtonian counterpart.

- To investigate the possible limitation of glycerol to generate strong foam, the higher concentrations of glycerol which could not generate strong foam were added to a 250 ppm polymer solution. The outcome is that these solutions indeed do generate strong foam, much stronger than that generated by the 250 ppm polymer solution on its own. It is concluded that the polymer increases the foamability, after which the generated foam is more stable due to the higher viscosity of the glycerol−polymer solution.

- Finally, the gas saturation inside the core is calculated on the basis of mass conservation. The solutions that were not capable of generating strong foam reach a much smaller maximum gas saturation. This implies that rather than the gas displacing a great amount of the fluid present and creating foam, it only displaces a bit of fluid. This could be explained by the concept earlier described where the weak foam is present but does not block all flow paths of the gas, hence leaving a flow path for the gas to shoot through.

All the conclusions indicate that glycerol can be considered a suitable and efficient alternative to polymers and be a solution to many limitations that polymers impose under reservoir conditions.

■ AUTHOR INFORMATION

Corresponding Authors

    Seyed Mojtaba Hosseini-Nasab − *School of Chemical, Petroleum and Gas Engineering, Iran University of Science and Technology, Tehran 13114-16846, Iran;* ● orcid.org/0000-0001-5429-1796; Email: Hosseininasab@iust.ac.ir

    Pacelli L. J. Zitha − *Department of Geoscience & Engineering, Reservoir Engineering Group, Delft University of Technology, Delft 2628 CD, Netherlands;* Email: P.L.J.Zitha@tudelft.nl

Authors

    Mohammad Rezaee − *Department of Petroleum Engineering, Amirkabir University of Technology, Tehran 1591634311, Iran*

    Martin Taal − *Chemical Development Department, Amsterdam 2132 LS, Netherlands*

Complete contact information is available at:
https://pubs.acs.org/10.1021/acsomega.2c04457

Notes

The authors declare no competing financial interest.

■ REFERENCES

(1) Burrows, L. C.; Haeri, F.; Cvetic, P.; Sanguinito, S.; Shi, F.; Tapriyal, D.; Goodman, A.; Enick, R. M. A literature review of CO2, natural gas, and water-based fluids for enhanced oil recovery in unconventional reservoirs. *Energy Fuels* **2020**, *34*, 5331−5380.

(2) Li, X.; Xiao, K.; Wang, R.; Li, X. Experimental Research on Enhanced Oil Recovery Methods for Gas Injection of Fractured Reservoirs Based on Microfluidic Chips. *ACS Omega* **2022**, *7*, 27382.

(3) Al-Mudhafar, W. J. From coreflooding and scaled physical model experiments to field-scale enhanced oil recovery evaluations: Comprehensive review of the gas-assisted gravity drainage process. *Energy Fuels* **2018**, *32*, 11067−11079.

(4) Zeng, Y.; Kamarul Bahrim, R. Z.; Groot, J. A.; Vincent-Bonnieu, S.; Groenenboom, J.; Mohd Shafian, S. R.; Abdul Manap, A. A.; Tewari, R. D.; Mohammadian, E.; Azdarpour, A.; Hamidi, H.; Biswal, S. L. Probing Methane Foam Transport in Heterogeneous Porous Media: An Experimental and Numerical Case Study of Permeability-Dependent Rheology and Fluid Diversion at Field Scale. *SPE J.* **2020**, *25*, 1697−1710.

(5) Emami, H.; Ayatizadeh Tanha, A.; Khaksar Manshad, A.; Mohammadi, A. H. Experimental Investigation of Foam Flooding Using Anionic and Nonionic Surfactants: A Screening Scenario to Assess the Effects of Salinity and pH on Foam Stability and Foam Height. *ACS Omega* **2022**, *7*, 14832−14847.

(6) Majeed, T.; Kamal, M. S.; Zhou, X.; Solling, T. A review on foam stabilizers for enhanced oil recovery. *Energy Fuels* **2021**, *35*, 5594−5612.

(7) Hosseini-Nasab, S. M.; Zitha, P. L. J. Investigation of chemical-foam design as a novel approach toward immiscible foam flooding for enhanced oil recovery. *Energy Fuels* **2017**, *31*, 10525−10534.

(8) Zitha, P. L. J. Foam drainage in porous media. *Transp. Porous Media* **2003**, *52*, 1−6.

(9) Zhao, F.; Wang, K.; Li, G.; Zhu, G.; Liu, L.; Jiang, Y. A Review of High-Temperature Foam for Improving Steam Flooding Effect: Mechanism and Application of Foam. *Energy Technol.* **2022**, *10*, 2100988.

(10) Conn, C. A.; Ma, K.; Hirasaki, G. J.; Biswal, S. L. Visualizing oil displacement with foam in a microfluidic device with permeability contrast. *Lab Chip* **2014**, *14*, 3968−3977.

(11) Aarra, M. G.; Murad, A. M.; Solbakken, J. S.; Skauge, A. Foam dynamics in limestone carbonate cores. *ACS Omega* **2020**, *5*, 23604−23612.

(12) Ding, L.; Jouenne, S.; Gharbi, O.; Pal, M.; Bertin, H.; Rahman, M. A.; Economou, I. G.; Romero, C.; Guérillot, D. An experimental investigation of the foam enhanced oil recovery process for a dual porosity and heterogeneous carbonate reservoir under strongly oil-wet condition. *Fuel* **2022**, *313*, 122684−122759.

(13) Hosseini-Nasab, S. M.; Padalkar, C.; Battistutta, E.; Zitha, P. L. Mechanistic modeling of the alkaline/surfactant/polymer flooding process under sub-optimum salinity conditions for enhanced oil recovery. *Ind. Eng. Chem. Res.* **2016**, *55*, 6875−6888.

(14) Simjoo, M.; Zitha, P. L. Modeling and experimental validation of rheological transition during foam flow in porous media. *Transp. Porous Media* **2020**, *131*, 315−332.

(15) Chen, H.; Li, Z.; Wang, F.; Li, S. Investigation on in situ foam technology for enhanced oil recovery in offshore oilfield. *Energy Fuels* **2019**, *33*, 12308−12318.

(16) Abdelaal, A.; Gajbhiye, R.; Al-Shehri, D. Mixed CO2/N2 foam for EOR as a novel solution for supercritical CO2 foam challenges in sandstone reservoirs. *ACS Omega* **2020**, *5*, 33140−33150.

(17) Petkova, R.; Tcholakova, S.; Denkov, N. D. Foaming and foam stability for mixed polymer−surfactant solutions: effects of surfactant type and polymer charge. *Langmuir* **2012**, *28*, 4996−5009.

(18) Xu, X.; Saeedi, A.; Liu, K. Laboratory studies on CO2 foam flooding enhanced by a novel amphiphilic ter-polymer. *J. Pet. Sci. Eng.* **2016**, *138*, 153−159.

(19) Hosseini-Nasab, S. M.; Zitha, P. L.; Mirhaj, S. A.; Simjoo, M.A New Chemical Enhanced Oil Recovery Method?. *SPE International Symposium on Oilfield Chemistry*; OnePetro, 2015.

(20) Zhou, W.; Xin, C.; Chen, S.; Yu, Q.; Wang, K. Polymer-enhanced foam flooding for improving heavy oil recovery in thin reservoirs. *Energy Fuels* **2020**, *34*, 4116−4128.

(21) Telmadarreie, A.; Trivedi, J. J. Post-Surfactant $\hbox{CO}_{2}$ CO 2 Foam/Polymer-Enhanced Foam Flooding for Heavy Oil Recovery: Pore-Scale Visualization in Fractured Micromodel. *Transp. Porous Media* **2016**, *113*, 717−733.

(22) Hanamertani, A. S.; Ahmed, S. Probing the role of associative polymer on scCO2-Foam strength and rheology enhancement in bulk and porous media for improving oil displacement efficiency. *Energy* **2021**, *228*, 120531.

(23) Gochev, G. Thin liquid films stabilized by polymers and polymer/surfactant mixtures. *Curr. Opin. Colloid Interface Sci.* **2015**, *20*, 115−123.

(24) Jones, S.; van der Bent, V.; Farajzadeh, R.; Rossen, W. R.; Vincent-Bonnieu, S. Surfactant screening for foam EOR: Correlation between bulk and core-flood experiments. *Colloids Surf., A* **2016**, *500*, 166−176.

(25) Andrianov, A.; Farajzadeh, R.; Mahmoodi Nick, M.; Talanana, M.; Zitha, P. L. Immiscible foam for enhancing oil recovery: bulk and porous media experiments. *Ind. Eng. Chem. Res.* **2012**, *51*, 2214−2226.

(26) Yu, Y.; Saraji, S. Supercritical CO2 Foam Stabilized by a Viscoelastic Surfactant in Fractured Porous Media: The Effect of Fracture Surface Roughness. *Energy Fuels* **2021**, *35*, 10051−10061.

(27) Skauge, A.; Solbakken, J.; Ormehaug, P. A.; Aarra, M. G. Foam generation, propagation and stability in porous medium. *Transp. Porous Media* **2020**, *131*, 5−21.

(28) Pu, W. F.; Wei, P.; Sun, L.; Jin, F. Y.; Wang, S. Experimental investigation of viscoelastic polymers for stabilizing foam. *J. Ind. Eng. Chem.* **2017**, *47*, 360−367.

(29) Zhong, H.; Li, Y.; Zhang, W.; Yin, H.; Lu, J.; Guo, D. Microflow mechanism of oil displacement by viscoelastic hydro-phobically associating water-soluble polymers in enhanced oil recovery. *Polymers* **2018**, *10*, 628.

(30) Rezaee, M.; Hosseini-Nasab, S. M.; Fahimpour, J.; Sharifi, M. New Insight on improving foam stability and foam flooding using fly-ash in the presence of crude oil. *J. Pet. Sci. Eng.* **2022**, *214*, 110534.

(31) Valdez, A. R.; Rocha, B. M.; da Fonseca Façanha, J. M.; de Souza, A. V.; Perez-Gramatges, A.; Chapiro, G.; Santos, R. W. Foam-Assisted Water−Gas Flow Parameters: From Core-Flood Experiment to Uncertainty Quantification and Sensitivity Analysis. *Transp. Porous Media* **2022**, *144*, 189−209.

(32) Alfazazi, U.; Thomas, N. C.; Alameri, W.; Al-Shalabi, E. W. Experimental investigation of polymer injectivity and retention under harsh carbonate reservoir conditions. *J. Pet. Sci. Eng.* **2020**, *192*, 107262.

(33) Kazempour, M.; Manrique, E. J.; Alvarado, V.; Zhang, J.; Lantz, M. Role of active clays on alkaline−surfactant−polymer formulation performance in sandstone formations. *Fuel* **2013**, *104*, 593−606.

(34) Majeed, T.; Kamal, M. S.; Zhou, X.; Solling, T. A review on foam stabilizers for enhanced oil recovery. *Energy Fuels* **2021**, *35*, 5594−5612.

(35) Alfazazi, U.; AlAmeri, W.; Hashmet, M. R. Experimental investigation of polymer flooding with low-salinity preconditioning of high temperature−high-salinity carbonate reservoir. *J. Pet. Explor. Prod. Technol.* **2019**, *9*, 1517−1530.

(36) Firozjaii, A. M.; Saghafi, H. R. Review on chemical enhanced oil recovery using polymer flooding: Fundamentals, experimental and numerical simulation. *Petroleum* **2020**, *6*, 115−122.

(37) Gbadamosi, A.; Patil, S.; Kamal, M. S.; Adewunmi, A. A.; Yusuff, A. S.; Agi, A.; Oseh, J. Application of Polymers for Chemical Enhanced Oil Recovery: A Review. *Polymers* **2022**, *14*, 1433.

(38) Scott, A. J.; Romero-Zerón, L.; Penlidis, A. Evaluation of polymeric materials for chemical enhanced oil recovery. *Processes* **2020**, *8*, 361.

(39) Vavra, E.; Puerto, M.; Biswal, S. L.; Hirasaki, G. J. A systematic approach to alkaline-surfactant-foam flooding of heavy oil: micro-fluidic assessment with a novel phase-behavior viscosity map. *Sci. Rep.* **2020**, *10*, 12930.

(40) Rezaeiakmal, F.; Parsaei, R. Visualization study of polymer enhanced foam (PEF) flooding for recovery of waterflood residual oil: Effect of cross flow. *J. Pet. Sci. Eng.* **2021**, *203*, 108583.

(41) Hosseini-Nasab, S. M.; Taal, M.; Zitha, P. L.; Sharifi, M. Effect of Newtonian and non-Newtonian viscosifying agents on stability of foams in enhanced oil recovery. Part I: under bulk condition. *Iran. Polym. J.* **2019**, *28*, 291−299.

(42) Hejna, A.; Kosmela, P.; Formela, K.; Piszczyk, Ł.; Haponiuk, J. T. Potential applications of crude glycerol in polymer technology−Current state and perspectives. *Renewable Sustainable Energy Rev.* **2016**, *66*, 449−475.

(43) Yu, Y.; Soukup, Z. A.; Saraji, S. An experimental study of in-situ foam rheology: effect of stabilizing and destabilizing agents. *Colloids Surf., A* **2019**, *578*, 123548.

(44) Hanamertani, A. S.; Ahmed, S. Probing the role of associative polymer on scCO2-Foam strength and rheology enhancement in bulk and porous media for improving oil displacement efficiency. *Energy* **2021**, *228*, 120531.

(45) Ahmed, S.; Elraies, K. A.; Forooozesh, J.; Bt Mohd Shafian, S. R.; Hashmet, M. R.; Hsia, I. C.; Almansour, A. Experimental investigation of immiscible supercritical carbon dioxide foam rheology for improved oil recovery. *J. Earth Sci.* **2017**, *28*, 835−841.

(46) Du, Y.; Zhu, Y.; Ji, Y.; Xu, H.; Zhang, H.; Yuan, S. Effect of salt-resistant monomers on viscosity of modified polymers based on the hydrolyzed poly-acrylamide (HPAM): A molecular dynamics study. *J. Mol. Liq.* **2021**, *325*, 115161.

(47) Dário, A. F.; Hortêncio, L. M.; Sierakowski, M. R.; Neto, J. C.; Petri, D. F. The effect of calcium salts on the viscosity and adsorption behavior of xanthan. *Carbohydr. Polym.* **2011**, *84*, 669−676.

(48) Zhou, H. X.; Pang, X. Electrostatic interactions in protein structure, folding, binding, and condensation. *Chem. Rev.* **2018**, *118*, 1691−1741.

(49) Nawrocki, G.; Karaboga, A.; Sugita, Y.; Feig, M. Effect of protein−protein interactions and solvent viscosity on the rotational diffusion of proteins in crowded environments. *Phys. Chem. Chem. Phys.* **2019**, *21*, 876−883.

(50) Goodarzi, F.; Zendehboudi, S. Effects of salt and surfactant on interfacial characteristics of water/oil systems: molecular dynamic simulations and dissipative particle dynamics. *Ind. Eng. Chem. Res.* **2019**, *58*, 8817−8834.

(51) Bai, B.; Leng, J.; Wei, M. A comprehensive review of in-situ polymer gel simulation for conformance control. *Pet. Sci.* **2022**, *19*, 189.

(52) Al-Shakry, B.; Skauge, T.; Shaker Shiran, B.; Skauge, A. Polymer injectivity: Investigation of mechanical degradation of enhanced oil recovery polymers using in-situ rheology. *Energies* **2018**, *12*, 49.

(53) Akbari, S.; Mahmood, S. M.; Nasr, N. H.; Al-Hajri, S.; Sabet, M. A critical review of concept and methods related to accessible pore volume during polymer-enhanced oil recovery. *J. Pet. Sci. Eng.* **2019**, *182*, 106263.

(54) Rock, A.; Hincapie, R. E.; Tahir, M.; Langanke, K.; Ganzer, L. On the role of polymer viscoelasticity in enhanced oil recovery: Extensive laboratory data and review. *Polymers* **2020**, *12* (10), 2276.

(55) Chauveteau, G. Rodlike polymer solution flow through fine pores: influence of pore size on rheological behavior. *J. Rheol.* **1982**, *26*, 111−142.

(56) Chauveteau, G.; Zaitoun, A.Basic rheological behavior of xanthan polysaccharide solutions in porous media: effects of pore size

and polymer concentration. In *Proceedings of the First European Symposium on Enhanced Oil Recovery*; Society of Petroleum Engineers: Bournemouth, England, Richardson, TX, 1981; pp 197−212.

(57) Sorbie, K. S.*Polymer-Improved Oil Recovery*; Springer Science & Business Media; 2013.

(58) Tahir, M.; Hincapie, R. E.; Be, M.; Ganzer, L. A Comprehensive Combination of apparent and shear viscoelastic data during polymer flooding for EOR evaluations. *World J. Text. Eng. Technol.* **2017**, *5*, 585−600.

(59) Peksa, A. E.; Wolf, K. H.; Zitha, P. L. Bentheimer sandstone revisited for experimental purposes. *Mar. Pet. Geol.* **2015**, *67*, 701−719.

(60) Vikingstad, A. K.; Skauge, A.; Høiland, H.; Aarra, M. Foam−oil interactions analyzed by static foam tests. *Colloids Surf., A* **2005**, *260*, 189−198.

(61) Xiong, J.; Zhao, Z.; Sun, W.; Liu, W. Foam Stabilization Mechanism of a Novel Non-cross-linked Foam Fracturing Fluid. *ACS Omega* **2021**, *6*, 32863−32868.

(62) Shi, S.; Li, J.; Yang, X.; Liu, C.; Liao, R.; Zhang, X.; Liao, J. Study on the Pressure Drop Variation and Prediction Model of Heavy Oil Gas-Liquid Two-Phase Flow. *Geofluids* **2021**, *2021*, 8813167.